Parcel-based urban land use classification in megacity using airborne LiDAR, high resolution orthoimagery, and Google Street View

Abstract

Urban land use information is increasingly important for a variety of purposes. With their increasing coverage and availability, airborne light detection and ranging (LiDAR) data, high resolution orthoimagery (HRO), and Google Street View (GSV) images are showing great potential for accurate land use classification. However, no study mapped land use in megacity using GSV-derived features or the three kinds of data together for land use classification. The main objectives of this study are (1) to test the performance of a parcel-based land use classification method using a Random Forest classifier with LiDAR data, HRO, and GSV images in a megacity, and (2) to explore the use of GSV in separating parcels of mixed residential & commercial buildings from other land use parcels. Two neighbouring community districts in Brooklyn, New York, were selected as the study area. Thirteen automatically-derived parcel features, including nine common parcel features and four GSV-derived parcel features, were used in land use classification. The average overall classification accuracy was 77.5%, with producer's accuracies exceeding 92% for single-family housing. Comparing the results of classifications with and without GSV-derived parcel features shows that GSV-derived parcel features on average contribute to the classification accuracy of mixed residential & commercial buildings by 10 percentage points, improving it from 41.3% to 51.4%. In general, the results show that even in a complex megacity, the parcel-based land use classification technique, with parcel features extracted from airborne LiDAR, HRO, and GSV, is able to discriminate among different land use classes, such as single-family house, commercial & industrial building, and open space & park, with acceptable accuracies, and that integrating GSV into classification improves the classification accuracy of some urban land use classes, especially mixed residential & commercial building.

Keywords: Urban land use; Classification; Megacity; Google Street View; LiDAR; Parcel feature.

1. Introduction

There were 34 megacities, defined as metropolitan areas with more than 10 million in population across the world by 2015 (Cox, 2015), in total having about 582 million in population. In order to have an in-depth understanding of the growth and development of megacities, accurate and timely information concerning urban land resources are needed (Moller-Jensen, 1997). Land use information in any city is important because it is essential to a variety of purposes (Wentz, Stefanov, Gries, & Hope, 2006), such as tax assessment, land use policy, city planning, zoning regulation, analysis of environmental processes and problems, and management of natural resources (Anderson, 1976; Treitz, Howarth, & Gong, 1992). Generally, local planning departments collect and update land use information by ground survey, visual interpretation of aerial images, or reference to other supplementary existing data (Anderson, 1976). For large-city areas, these traditional ways of collecting and updating land use data could be extremely laborious, costly, and time consuming (Wu, Qiu, Usery, & Wang, 2009).

Due to recent technological advancement in remote sensors and image analysis tools, high spatial resolution imagery has shown a great capacity for land cover/use classification in urban areas (Barr & Barnsley, 2000). The nature of urban land use is mainly defined in terms of social economic functionality (Barnsley & Barr, 1997; Bauer & Steinnocher, 2001), so recognition of land use by spectral reflectance from optical remote sensing (RS) images is still a major challenge (Donnay & Unwin, 2001). Another challenging problem in mapping land use in urban areas is the complexity of the urban landscape (Aubrecht, Steinnocher, Hollaus, & Wagner, 2009).

To overcome these difficulties, researchers have developed a variety of land-use classification methods. The existing methods of land-use classification may be grouped into two categories in terms of

land use units: one uses pixel-based approaches and the other uses region-based approaches. Delimitation of land-use regions or parcels is an initial requirement of analyses in the region-based approaches, several ways have been developed to divide an urban area, such as manual delineation (Herold, Liu, & Clarke, 2003), use of GIS data (e.g., administrative boundary, parcel boundary, roads) (Wu, Silván-Cárdenas, & Wang, 2007), and image segmentation (Platt & Rapoza, 2008). Then urban land use can be classified based on the differences in spatial distributions and patterns of buildings, other built structures, vegetation cover, and other features within parcels (Bauer & Steinnocher, 2001). Region-based approaches have been widely used in land use classification. For example, Bauer and Steinnocher (2001) used an object-oriented rule-based classifier for urban land use classification over IKONOS images. Wu, Silván-Cárdenas, and Wang (2007) employed a region-based approach with a decision tree classifier for urban land use classification based on 12 parcel features and obtained a relatively high accuracy in a middle-sized city. By taking up to 50 parcel features into account and using the same region-based approach in the same study area, Wu, Qiu, Usery, and Wang (2009) further improved the accuracy of land use classification.

However, little effort has been spent in testing the effectiveness of region-based land-use classification approaches in megacities, which are probably the most complicated landscapes because of their substantial three dimensional (3D) components and mixed land use classes (e.g., mixed residential & commercial buildings). To deal with the complexity of megacity landscapes, in addition to high resolution orthoimagery (HRO) and LiDAR, Google Street View (GSV) images were first used in this study to improve land use classification. While LiDAR is able to provide informative 3D data of parcels, GSV enables us to horizontally observe parcels at street-level. Recently, GSV images were used in environmental and social researches, such as auditing neighbourhood environments (Rundle et al., 2011; Bentley, McCutcheon, Cromley, & Hanink, 2016), assessment of sidewalk accessibility (Hara & Froehlich, 2013), urban greenery assessment (Li et al., 2015).

In this study, a region-based approach is used with parcel boundary data for land use classification in a megacity: New York. Parcel boundaries are reasonable boundaries of urban land use classes because urban land use is more of a socio-economic function than a natural one. Thus the term “parcel-based” was used to specify the urban land use classification method in this study. Additionally, using a region-based approach allows data obtained from different sensors to be configured consistently even though these data have various scales, resolutions, and visions. Particularly, with increasing coverage and more availability, airborne LiDAR data, HRO, and GSV images may have great potential for accurate up-to-date urban land use classification using region-based approaches. The objectives of this study are: (1) to investigate the performance of a parcel-based urban land use classification method using a Random Forest classifier with LiDAR data, HRO, and GSV images in a megacity; (2) to test the importance of different parcel features for urban land use classification; and (3) to exam the effectiveness of GSV images for improving accuracy of urban land use classification under a complex megacity background.

2. Study Area and Data

2.1. Study Area

New York City (NYC) is the most populous city in the United States (US) (U.S. Census Bureau, 2016) and also one of the most populous metropolises on the Earth (Worldatlas, 2016). The city has five boroughs: Brooklyn, Queens, Manhattan, the Bronx, and Staten Island. Brooklyn, which coincides with Kings County, is the most densely populated among these five boroughs, with 2.5 million residents and 1 million housing units in 2014, according to 2010-2014 American Community Survey 5-Year Estimates. Brooklyn is located at the south-western end of Long Island. Two community districts, covering 12.9 square kilometres, in the central part of Brooklyn were chosen as our case study area (Fig. 1).

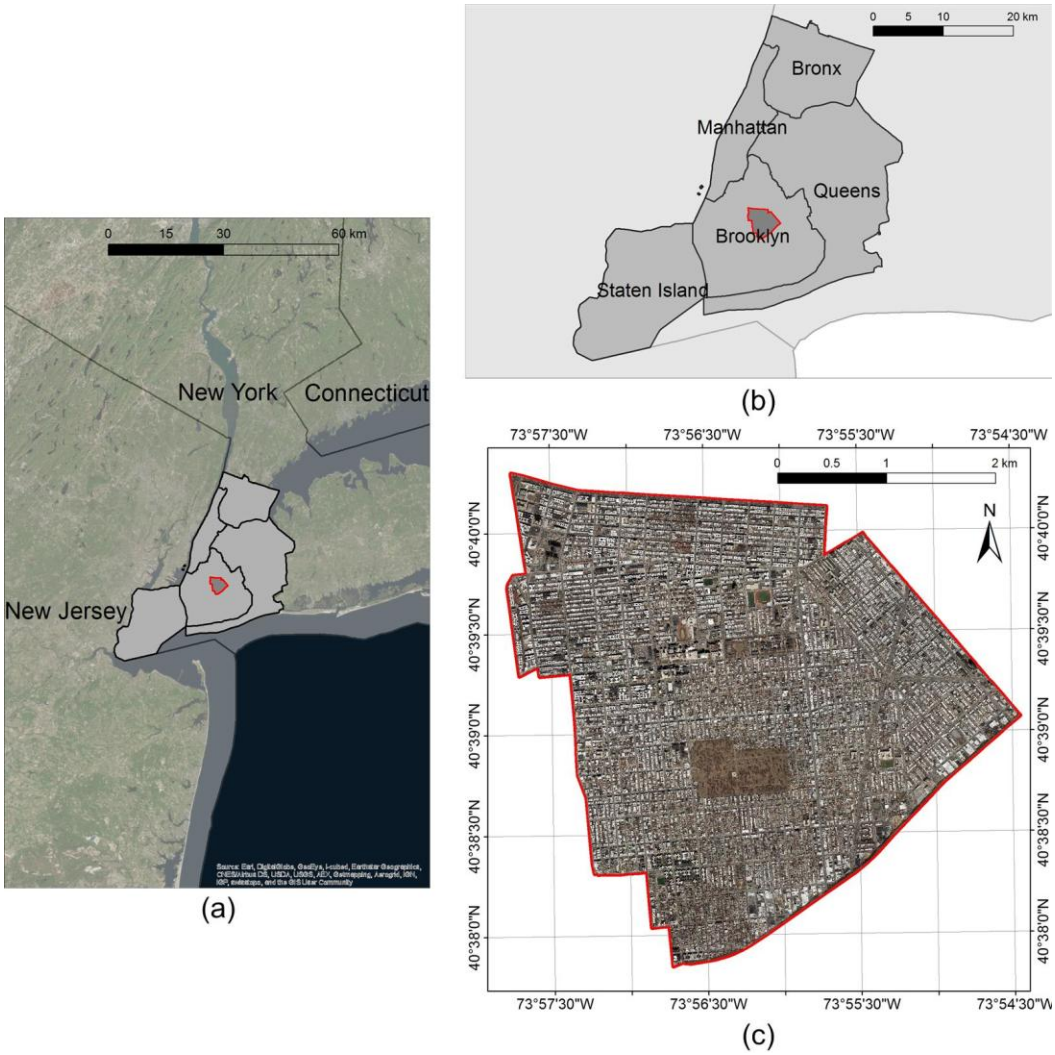

Fig. 1. The study area – the central part of Brooklyn: (a) location of the study area in New York City; (b) New York City consists of five boroughs; and (c) a true-colour composite of the high resolution orthoimagery (RGB = 4, 3, 2) for the study area. The image was acquired on April 01, 2014, with a spatial resolution of 0.5 feet. The latitude and longitude of the upper left corner of the image is 40°40'25.467"N, 73°57'53.833"W.

2.2. GIS Data

We obtained parcel boundary data and study area boundary from the NYC Department of City Planning (DCP), and street data from the New York State GIS Program Office, in the "NAD_1983_2011_StatePlane_New_York_Long_Isl_FIPS_3104_Ft_US" projected coordinate system. The parcel boundary data are in vector polygon format, with 83 different social, administrative, and geographic attributes. The corresponding land use inventory information at parcel level in the study area is used as reference data. The parcel boundary data originally have a total of 11 land use classes, which were converted into 7 classes (Table 1) with minor classes merged with functionally similar major classes.

Table 1

Description of related land use classes in the study area.

Land use class (before merging)	Land use ID (before merging)	Land use class (after merging)	Land use ID (after merging)	Descriptions

One & two family buildings	1	Single-family house	L1	Single-family detached home, two-unit dwelling group, and duplex
Multi-family walk-up buildings Multi-family elevator buildings	2 3	Multi-family residential building	L2	Two-flat, three-flat, four-flat, townhouse, apartment building, and apartment community
Public facilities & institutions	8	Public facility & institution	L3	Hospital, government services, and educational facilities
Mixed residential & commercial buildings	4	Mixed residential & commercial building	L4	Mixed use building that has spaces for both commercial and residential use
Commercial & office buildings Industrial & manufacturing Transportation & utility	5 6 7	Commercial & industrial building	L5	Retail and general merchandise, shopping mall, restaurant, entertainment, manufacturing, warehousing, equipment sales and service, auto service, and multi-story car park
Open space & outdoor recreation Vacant land	9 11	Park & open space	L6	Public parks, urban parks, recreational facilities, golf courses, reservoir, and vacant space
Parking facilities	10	Parking facility	L7	Outdoor parking facility

The street data are also in vector polyline format, including vector lines of public/private streets. New York City consists of 70 community districts. Two community districts in Brooklyn were chosen and merged as the study area. All of GIS data used in this study were obtained from multiple sources compiled by different agencies, so there is no absolute guarantee of their completeness, accuracy, content, or fitness for any particular purpose. Some pre-processing was conducted. For example, parcels of road, highway, and railway in the parcel boundary data were removed because they are not relevant to this study. Moreover, some obvious out-of-date mistakes in the parcel boundary data were corrected by editing vertices. For example, the parcel of Holy Cross Cemetery still covers half of adjacent E 47th Street in the original data. Finally, the *Project* tool from ArcGIS tool box was used to project these GIS data into the "WGS_1984_UTM_zone_18N" projected coordinate system in order to match image data.

2.3. Remotely Sensed Data

2.3.1 Airborne Light Detection and Ranging (LiDAR)

In this study, LiDAR dataset was downloaded in LAS format and "WGS_1984_UTM_zone_18N" projected coordinate system, from National Oceanic and Atmospheric Administration (NOAA) via a Data Access Viewer (https://coast.noaa.gov/dataviewer/#/lidar/search/). (The LAS format is a public data format for the interchange of 3-dimensional point cloud data between data users [Version, 2009].) The LiDAR data were acquired for 304 square miles in New York State, by contractor Woolpert, Inc., from August 5 to August 15, 2013 and from March 21 to April 21, 2014, respectively (NOAA, 2015). The dataset has an overall density of 3.6 returns/m^2. The dataset was compiled to meet 0.42 meters horizontal accuracy at the 95 percent confidence level. According to the Consolidated Vertical Accuracy test result, the dataset has 0.116 meters consolidated vertical accuracy at the 95 percent confidence level for all land cover categories combined (NOAA, 2015). In order to keep the horizontal accuracy of the LiDAR dataset, it was resampled to 0.5 meters for further raster data processing with other aerial images.

2.3.2 High Resolution Orthoimagery (HRO)

High Resolution Orthoimages used in this study were obtained in the "NAD_1983_2011_StatePlane_New_York_Long_Isl_FIPS_3104_Ft_US" projected coordinate system from the United States Geological Survey (USGS) by EarthExplorer (http://earthexplorer.usgs.gov/). These aerial images were acquired from April 1 to April 25, 2014, with a pixel resolution of 0.1524 meters (i.e. 0.5 feet), including red, green, blue, and near infrared bands. We resampled these aerial images to the same spatial resolution as LiDAR raster images. To match the projected coordinate system of LiDAR, we also projected resampled HRO into the "WGS_1984_UTM_zone_18N" projected coordinate system.

2.3.3 Google Street View (GSV) Images

GSV images are available via Google Maps APIs. The GSV image API enables users to obtain a static (non-interactive) Street View panorama through a standard HTTP request with required URL parameters (Google, 2016). These parameters are *size*, *location*, *heading*, *fov*, *pitch*, and *key*. So far there has been no research using derived information (e.g., text information) from GSV images for improving land use classification. Therefore, in order to minimize the effect of zoom level on derived information caused by the varying distance between a building and the street view vehicle, three different horizontal field view angles (i.e., *fov*, which represents the level of zoom), 30, 45, and 60 degrees with default 5 degree vertical angle value (i.e., *pitch*) of the camera relative to the street view vehicle, were chosen when requesting GSV images for each parcel. To have corresponding GSV images for each parcel in the study area, we used the *Near* tool from ArcGIS toolbox to extract the *x*- and *y*-coordinates (i.e., *location*) of the nearest geo-location from Street Map for each parcel, and a near angle (i.e., *heading*) to measure the direction of the parcel to this nearest geo-location (Fig. 2(a)). Then the x- and y-coordinates of the nearest geo-location were converted to latitude and longitude coordinates. We developed a Python script to read the coordinates of each parcel and download the GSV images at that site by parsing GSV URL automatically (Fig. 2(b) and Fig. 2(c)). The requested GSV images did not include capture time, but they were acquired by Google from 2011 to 2014 based on sampling observation.

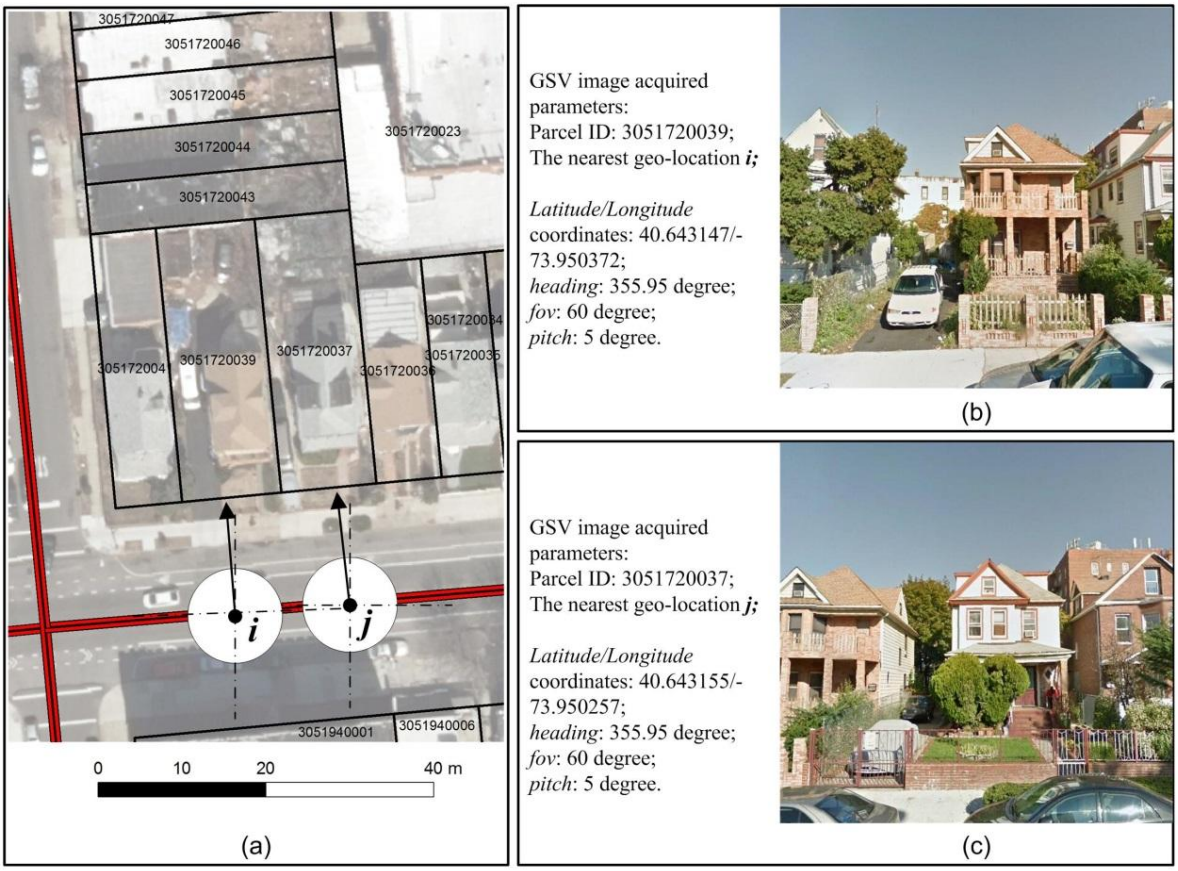

Fig. 2. GSV image downloading. (a) Using the *Near* tool to locate the nearest geo-location ***i*** and ***j*** from Street Map for two parcels, whose BBL (BBL is a concatenation of the borough code, tax block and tax lot) codes are 3051720039 and 3051720037, respectively. Based on x- and y-coordinates of extracted ***i*** and ***j***, we requested two GSV images for these two parcels: (b) a GSV image was downloaded from GSV URL for parcel 3051720039; (c) a GSV image was downloaded from GSV URL for parcel 3051720037.

3. Methods

In this study, thirteen parcel features (Table 2) were chosen as input variables in a Random Forest classifier for land use classification (Fig. 3). They include nine common parcel features: *parcel size, number of buildings, maximum of building areas, standard deviation (STD) of building areas, percentage of total building area, maximum of building story numbers, STD of building story numbers, average of normalized difference vegetation index (NDVI), STD of NDVI*. These parcel features were selected on the basis of related previous researches and empirical considerations (Fig. 4). For example, a study found that building-relevant features are the major discriminant factors between land use types with parcel-relevant features as secondary discriminant factors (Wu, Silván-Cárdenas, & Wang, 2007). Compared with other urban land-use classes, single-family house parcels tend to have smaller parcel size, smaller maximum of building areas, and lower maximum of building story numbers. Both apartment communities and public facilities have a larger number of buildings than parcels in any other land use class have, but apartment communities have more uniform building heights (Fig. 4(b-2)). Thus, STD of building story numbers can distinguish apartment communities from the others. Using the average of NDVI and STD of NDVI can identify park & open space because this land-use type tends to have higher coverage of vegetation (Fig. 4(f-3)). Using maximum of building areas, maximum of building story numbers and percentage of total building area can be helpful in recognizing commercial & industrial buildings because their parcels usually have large but low-rise buildings with large parking areas (Fig. 4(e-2)) (Wu, Silván-Cárdenas, & Wang, 2007).

The rest four parcel features were automatically detected and derived from GSV images (i.e., GSV-derived parcel features): *length of detected text from fov 30 GSV image*, *length of detected text from fov 45 GSV image*, *length of detected text from fov 60 GSV image*, and *index of English words from all detected text from GSV images*. Mixed residential & commercial buildings have spaces for both commercial and residential uses. Therefore, it is difficult to distinguish mixed residential & commercial buildings from either single-family houses or multi-family residential buildings because they have a lot of common building-relevant features, parcel-relevant features, and vegetation features (Fig. 4(a-1), (a-2), (a-3), (d-1), (d-2), and (d-3)). We propose to extract text information from GSV images in order to improve the accuracy of distinguishing mixed residential & commercial buildings from single-family houses and multi-family residential buildings, because the former have shop signs but the latter do not have (Fig. 4(a-4) and (d-4)).

Table 2
Description of selected parcel features.

No.	Parcel feature	Feature symbol	Description
1	Parcel size	**PF-1**	Area of a parcel
2	Number of buildings	**PF-2**	Number of detected buildings within a parcel
3	Maximum of building areas	**PF-3**	The largest area among the areas of buildings within a parcel
4	STD of building areas	**PF-4**	Standard deviation of areas of buildings within a parcel
5	Percentage of total building area	**PF-5**	Percentage of total building area within a parcel
6	Maximum of building story numbers	**PF-6**	The largest story number among the story numbers of buildings within a parcel
7	STD of building story numbers	**PF-7**	Standard deviation of building story numbers within a parcel
8	Average of NDVI	**PF-8**	Mean of NDVI values of pixels in a parcel
9	STD of NDVI	**PF-9**	Standard deviation of NDVI values of pixels in a parcel
10	Length of detected text from *fov* 30 GSV image	**PF-10**	Length of detected text derived from a requested GSV image with a horizontal field view angle as 30
11	Length of detected text from *fov* 45 GSV image	**PF-11**	Length of detected text derived from a requested GSV image with a horizontal field view angle as 45

12	Length of detected text from *fov* 60 GSV image	**PF-12**	Length of detected text derived from a requested GSV image with a horizontal field view angle as 60
13	Index of English word from all detected texts from GSV images	**PF-13**	Sum of existence of English word among detected texts from *fov* 30 GSV image, *fov* 45 GSV image, and *fov* 60 GSV image for a parcel (ranging from 0 to 3)

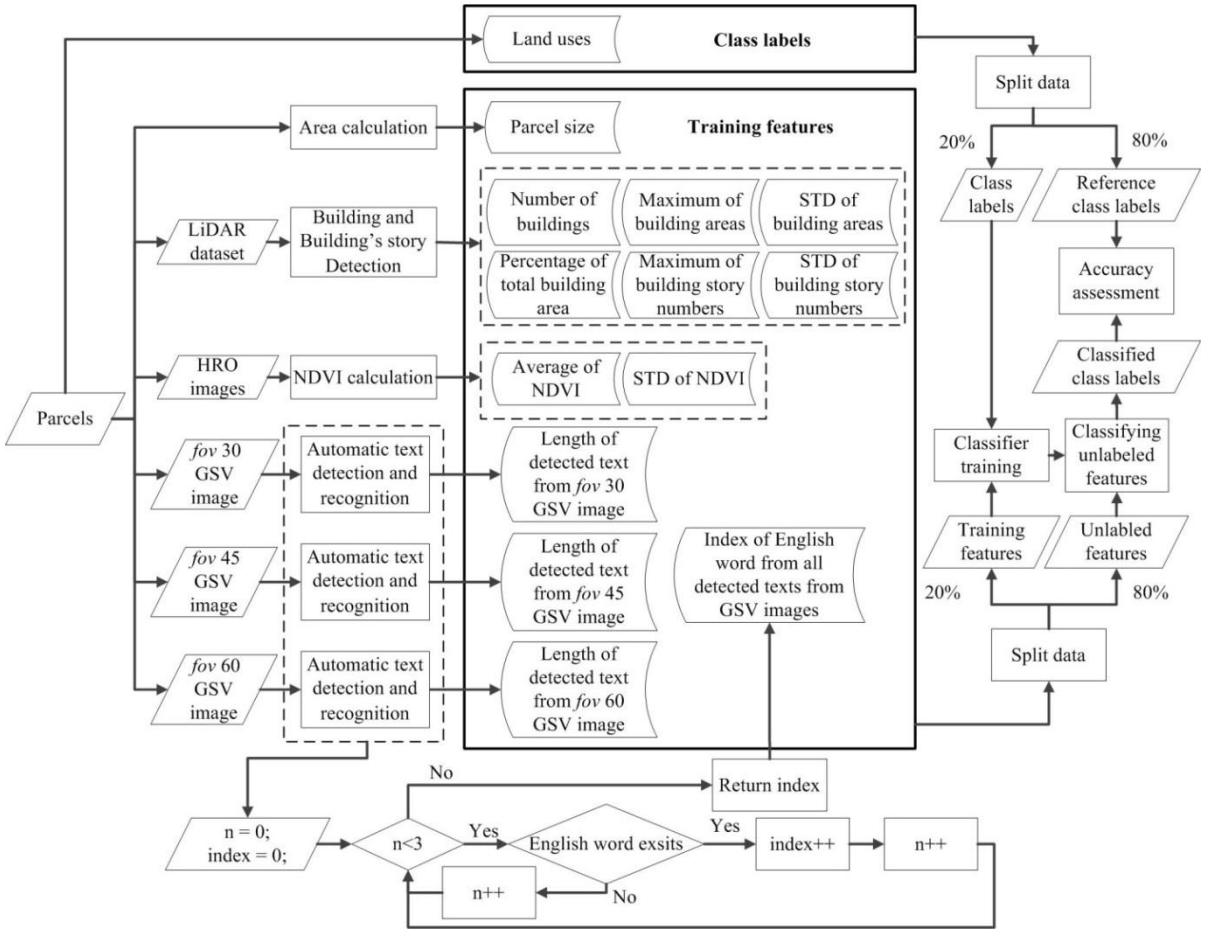

Fig. 3. A flowchart of the whole procedure from parcel feature calculation to classifier training to accuracy assessment.

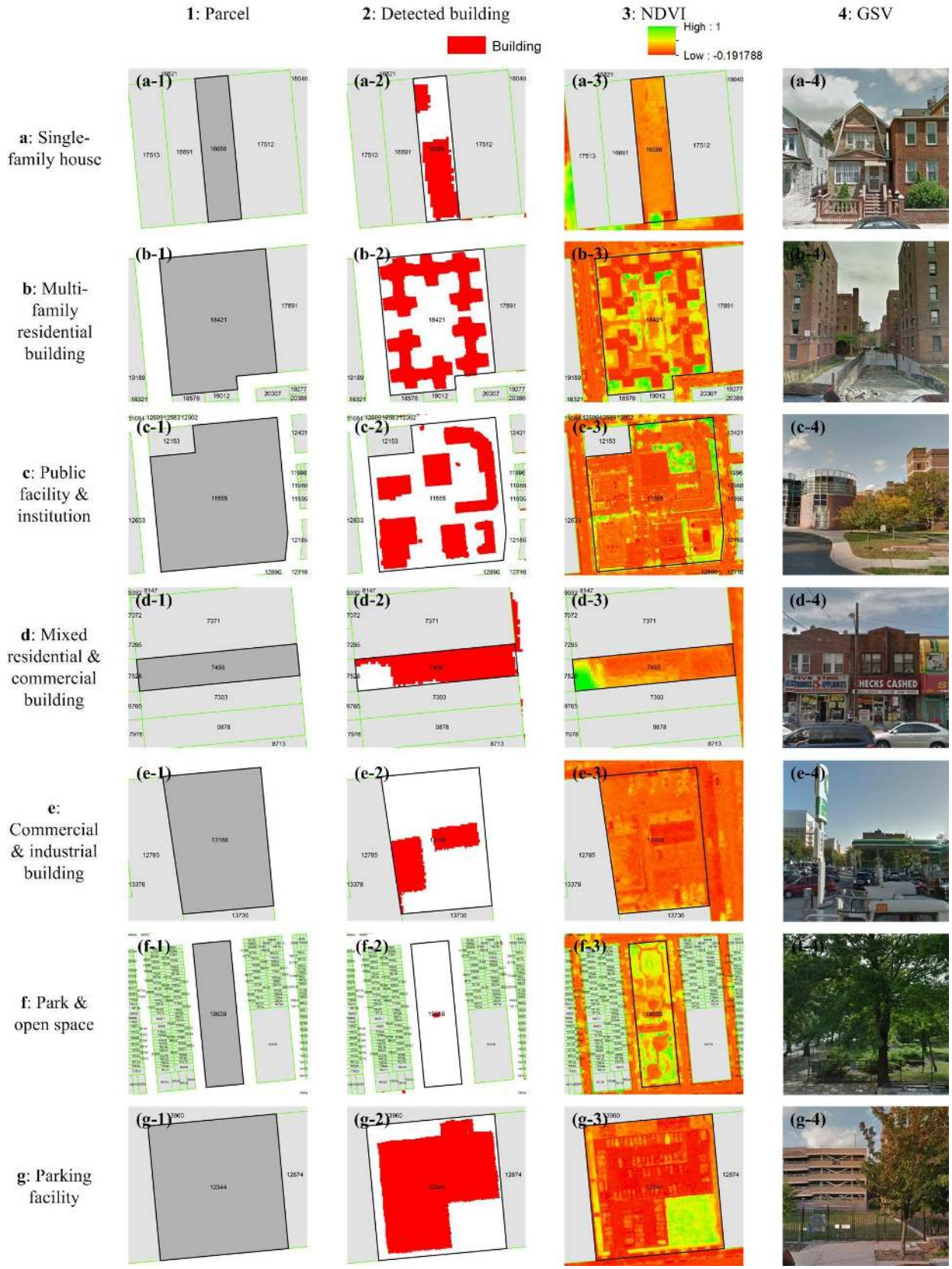

Fig. 4. Examples of used data for seven land use types.

In this study, only parcel size was calculated from parcel boundary data directly. The calculation of other 12 parcel features is described in following sections. After deriving the totally thirteen parcel features of each parcel from input data mentioned above, we trained a Random Forest classifier by using these derived parcel features and known land-use labels from the randomly selected 20 percent of all parcels. Then, the Random Forest Classifier classified the rest of parcels into the seven land use types. We chose the Random Forest Classifier in this study because we found that this classifier generated the best result after comparing it with some other common classifiers (e.g. Support Vector Machine and Decision Tree) in a test. Accuracy of land use classification was validated by the land use information of the 80 percent of parcels that were classified in the former step. Five random seeds (611, 1924, 3391, 6763, and 9930, all generated by a random number generator) were used to initialize a pseudorandom number generator when randomly selecting 20 percent of all parcels as training samples (Table 3). Accuracies were validated using the other 80 percent of the parcels (Table 3). Therefore, 5 different data groups were used as inputs to conduct classification and validation.

Table 3
Number of training parcels and test parcels for each land use type.

Random seed number	Parcel	Number of parcels for different land use types							
		L1	**L2**	**L3**	**L4**	**L5**	**L6**	**L7**	Total
611	Training parcels	3298	1036	86	366	131	80	66	5063
	Test parcels	12910	4243	334	1478	622	262	209	20058
	Total parcels	16208	5279	420	1844	753	342	275	25121
1924	Training parcels	3193	1030	79	393	143	69	48	4955
	Test parcels	13015	4249	341	1451	610	273	227	20166
	Total parcels	16208	5279	420	1844	753	342	275	25121
3391	Training parcels	3306	1054	92	378	142	62	66	5100
	Test parcels	12902	4225	328	1466	611	280	209	20021
	Total parcels	16208	5279	420	1844	753	342	275	25121
6763	Training parcels	3162	1123	79	385	142	68	50	5009
	Test parcels	13046	4156	341	1459	611	274	225	20112
	Total parcels	16208	5279	420	1844	753	342	275	25121
9930	Training parcels	3251	1050	92	338	161	68	58	5018
	Test parcels	12957	4229	328	1506	592	274	217	20103
	Total parcels	16208	5279	420	1844	753	342	275	25121

* **L1**: Single-family house; **L2**: Multi-family residential building; **L3**: Public facility & institution; **L4**: Mixed residential & commercial building; **L5**: Commercial & industrial building; **L6**: Park & open space; **L7**: Parking facility.

3.1 Normalized Difference Vegetation Index (NDVI)

The Normalized Difference Vegetation Index (NDVI) is a widely used measurement of vegetation because of its high reflectance in the near-infrared spectral region but low reflectance in the red spectral region (Song, 2005; Li et al., 2014). The value of the NDVI is generally between –1 and +1. It is close to +1 if a pixel is covered by vegetation. NDVI is calculated as (Tucker, 1979)

$$NDVI = \frac{R_{NIR} - R_{red}}{R_{NIR} + R_{red}} \quad (1)$$

where R_{NIR} is the reflectance in the near-infrared band and R_{red} is the reflectance in the red band.

3.2 Building Detection and Building Story Estimation

Point cloud of the LiDAR dataset was classified into some classes (in this data, they are default, ground, noise, water, ignored ground, overlap default, and overlap ground) during pre-processing. For the

bare-earth (i.e. ground) and non-ground LiDAR points, a manual Quality Assurance/Quality Control step was taken to verify their quality by removing artefacts (NOAA, 2015). Therefore, non-ground LiDAR points included artefacts (e.g., buildings), waterbody, and others (e.g., conifers and evergreens). However, the study area has no waterbody. Based on these characteristics of LiDAR data, a ground binary raster image (1: ground; 0: undecided) was produced by converting LiDAR ground points in LAS format into 0.5 meter pixels. Then, a moving window with the Boolean operation "and" and a radius of five pixels (i.e. 2.5 meters) was used to fill the gaps among ground pixels using the ground pixels located in each quadrant neighbourhood (Fig. 5). Finally, only relatively large patches (larger than 5 × 5 meters) with aggregative label-undecided pixels were left and regarded as buildings, and other label-undecided pixels surrounded by ground pixels were changed into ground pixels in the raster image. There were 1951 pixels selected randomly for building detection validation. The overall accuracy of building detection was 95.03%. Some mistakes might be attributed to some objects that have high elevation and do not have multiple laser returns and ground laser return, such as non-deciduous trees with dense canopy, trash piles, and truck trailers.

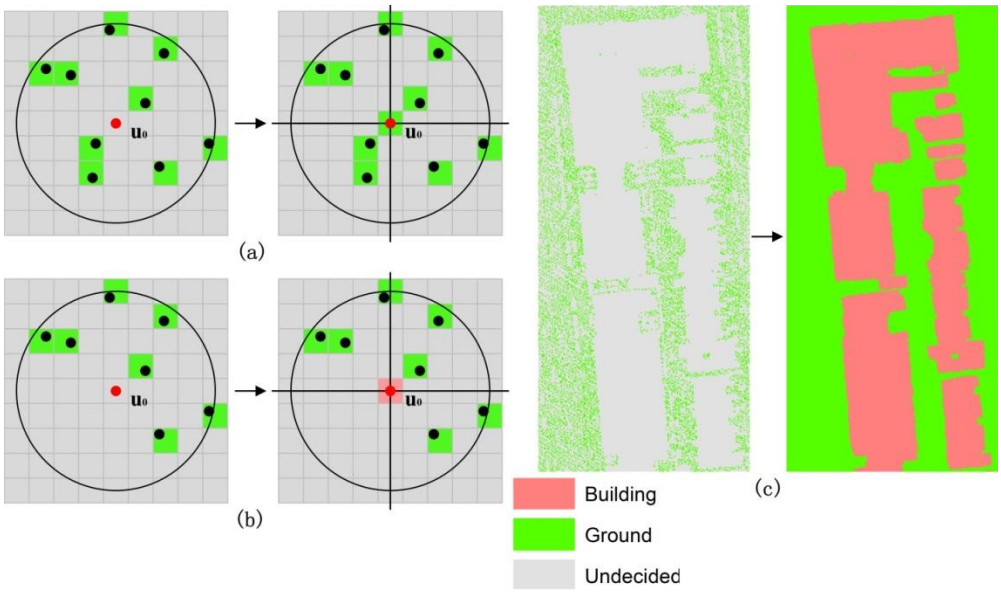

Fig. 5. Moving window with a radius for a quadrantal neighborhood for filling the gaps in LiDAR data. (a) LiDAR ground points (marked as black dots) are converted into ground pixels (marked as green pixels). The search area with a radius of 2.5 meters is used for seeking the nearest neighbors to decide whether a gap pixel's label is ground or building at the pixel $\mathbf{u}_0$. Because there is at least one ground pixel per quadrant, the pixel $\mathbf{u}_0$ is labelled as a ground pixel. (b) Because there is no LiDAR ground point located in the southwestern quadrant of the neighborhood, the gap pixel $\mathbf{u}_0$ will be labelled as a building pixel (marked as pink pixels). (c) A filled ground binary raster image was produced by the moving window.

As opposed to methods that derive building heights by subtracting ground surface elevation data from LiDAR elevation data, we derived building heights by subtracting the elevation of each parcel from the mean of LiDAR elevations at pixels within detected buildings. Usually researchers divide LiDAR points into ground (terrain) and non-ground (non-terrain) points by filtering. Then, an interpolation method is used to generate a digital elevation model (DEM) as ground surface elevation data (Liu, 2008). However, in megacities, parcels tend to be flat and their elevations may be very different from neighbouring parcels but uniform within themselves. We extracted elevation values of pixels for parcels with a 10 pixels (i.e. 5 meters) buffer but not including pixels in other parcels. For example, only elevation values of pixels from the front of a parcel would be extracted only if the front side of the parcel faces a street (Fig. 6). The median value of 5% of the smallest elevation values was used to represent the elevation of a parcel in order to avoid overestimation l. This is because that there may be some trees, cars and artefacts located at

the front of a parcel other than the street surface (Priestnall, Jaafar, & Duncan, 2000). Finally, derived building heights were converted to the storey numbers of buildings using 3 meters per storey.

Fig. 6. Extraction areas (shown with red boundaries) for elevation values of pixels within a 10 pixels (i.e. 5 meters) buffer around parcels (shown with green boundaries).

3.3. Automatic Detection and Recognition of Texts in GSV Images

The basic assumption in using GSV images in distinguishing mixed residential & commercial buildings (Fig. 7) from single-family houses and multi-family residential buildings (Fig. 8) is that shop signs of mixed residential & commercial buildings can be detected and recognized as texts from the corresponding GSV images. The Computer Vision System Toolbox of MATLAB (version: R2016a) was used to conduct robust text detection in GSV images. Firstly, the maximally stable extremal regions (MSER) feature detector was used to detect potential text regions. The MSER algorithm is able to detect most of the text regions, but it can also detect many other non-text regions in the image. Therefore, we removed non-text regions using a rule-based method to filter non-text regions based on geometric properties. We chose thresholds for these geometric properties based on the recommendation of example codes (http://www.mathworks.com/help/vision/examples/automatically-detect-and-recognize-text-in-natural-images.html) in MATLAB. Secondly, *Stroke Width* (SW) was used to further discriminate between text and non-text. The SW is a metric for measuring the width of the curves and lines that make up a character (MathWorks, 2016). Text regions tend to have little SW variation, whereas non-text regions tend to have larger SW variation (MathWorks, 2016). Thirdly, to extract more meaningful information than just individual characters, detected text regions were merged into text lines for obtaining final text detection results by forming a bounding box around text regions and expanding the bounding box (MathWorks, 2016). Finally, the *Optical character recognition* (OCR) function was used to recognize the text within each bounding box.

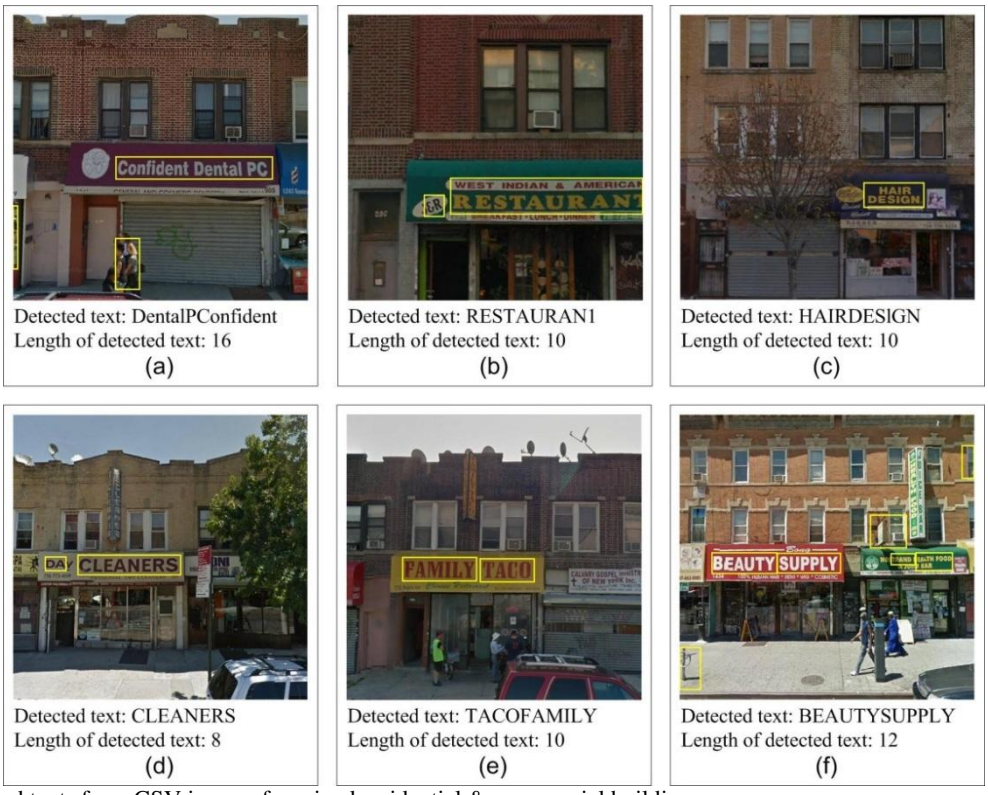

Fig. 7. Detected texts from GSV images for mixed residential & commercial buildings.

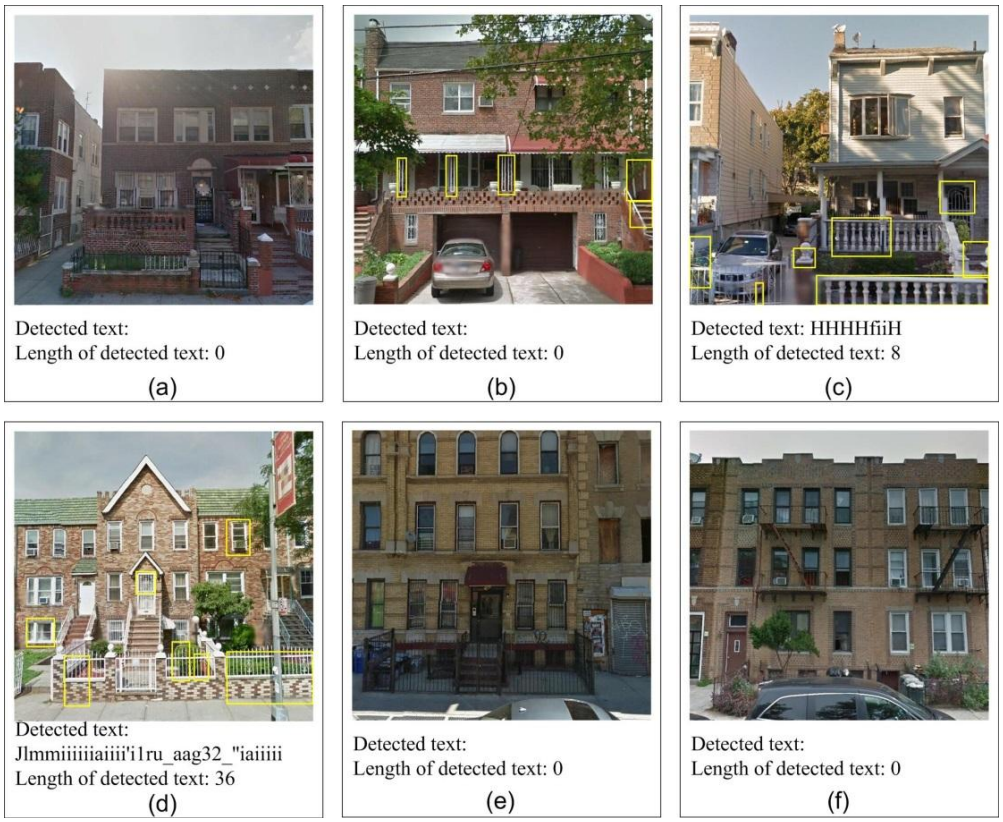

Fig. 8. Detected texts from GSV images for single-family houses and multi-family residential buildings.

3.4. Random Forest Classifier

The Random Forest (RF) classifier is a powerful machine learning classifier, which was initially developed by Breiman (2001) (Rodriguez-Galiano, Ghimire, Rogan, Chica-Olmo, & Rigol-Sanchez, 2012). Different from the Decision Tree (DT) classifier, the RF classifier builds multiple decision trees. Moreover, rather than training each tree on all inputs as the DT classifier does, the RF classifier builds each tree using different partial data from all inputs (also known as bootstrapped samples) (Grus, 2015). Rather than using all the remaining attributes, the RF classifier starts from choosing a random subset of them and then splits them based on an optimum choice (Grus, 2015). When classifying a new input vector, the RF classifier determines the final classification based on a majority vote (Gislason, Benediktsson, & Sveinsson, 2004). In this study, we used the RF classifier from the Scikit-learn Machine Learning Library (scikit-learn.org/stable/) for the Python programming language.

4. Results and Analyses

4.1 Classification Results Using Nine Common Parcel Features

Fig. 9(a) shows the land use classification based on the nine common parcel features (without the four GSV-derived parcel features) from training samples randomly selected using the random seed number 611. Fig. 9(b) shows incorrectly classified land-use class labels. The overall accuracies (OAs) of the classifications with different random number seeds were given in Table 4. Without the parcel features from GSV images, OAs range from 75.9% to 76.7%. The averaged OA of land use classifications based on the nine common parcel features is 76.3%. The accuracy assessment (Table 4) shows that the single-family house land use class has the highest producer's and user's accuracies (above 91% and 81%, respectively), compared with other land use classes. This can be explained by the relatively uniform small parcel size and single low-rise buildings of this land-use class (Wu, Qiu, Usery, & Wang, 2009). The land-use class for park & open space has the second highest average producer's and user's accuracies (greater than 68%) among all land-use classes. This may be because parcels for park & open space are more likely to have large areas and high percent vegetation cover. Next to the class of park & open space is the class of commercial & industrial building, of which the average producer's and user's accuracies are above 61% and 63%, respectively. Many parcels of the commercial & industrial building class were misclassified as single-family house, multi-family residential building, and mixed residential & commercial building (Table 5). The reason may be that, in a megacity, many small businesses or light industrial buildings, such as one or two story garages and convenient stores, have very similar parcel sizes and building features. However, for those large commercial & industrial buildings, they were easily classified correctly (see the lower right of Fig. 9(b)). Average producer's and user's accuracies for multi-family residential buildings are around 49.8% and 63.4%, respectively. It is not surprising that almost half of the multi-family residential parcels were misclassified as single-family houses (Table 5). This is because in the study area multi-family residential buildings mainly consist of two-flat, three-flat, and four-flat buildings, and these two- to four-flat multi-family residential buildings are similar to single-family houses in terms of parcel- and building-relevant characteristics. Average producer's and user's accuracies for mixed residential & commercial buildings are 41.3% and 57.9%, respectively, which can be explained by the similarity between residential buildings and mixed residential & commercial buildings in terms of parcel characteristics (e.g., in study area, some residential buildings and mixed residential & commercial buildings are two-story height single buildings with similar parcel size and building size). Parking facility and public facility & institution are two minor land-use classes here, with quite low classification accuracies due to some reasons discussed below.

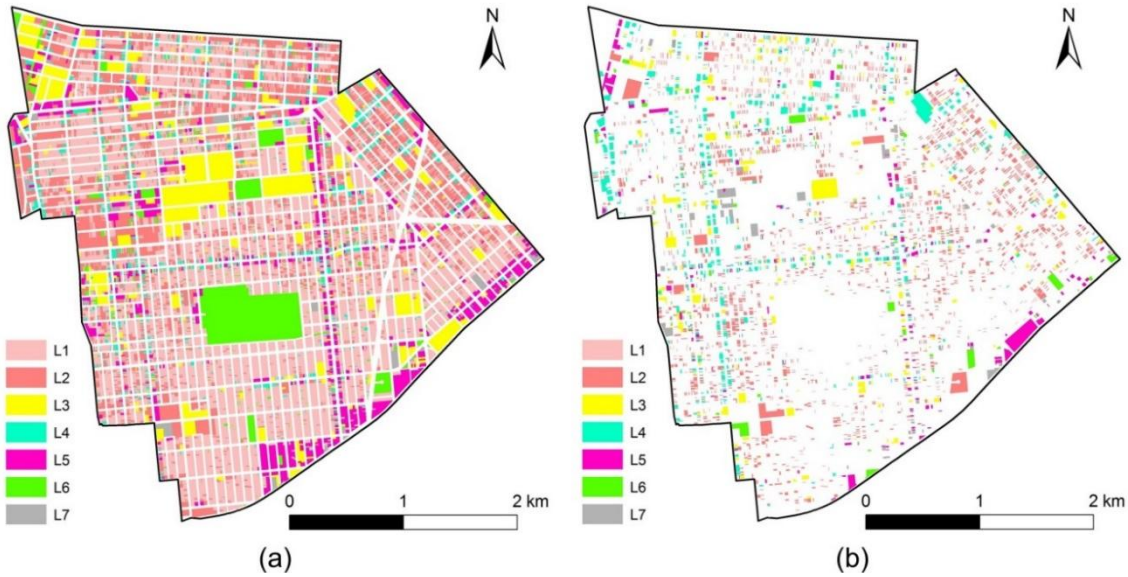

Fig. 9. (a) Land use classification based on nine common parcel features and the training samples randomly selected using the random seed number 611. (b) Corresponding land use misclassification.

Table 4
Accuracy assessment of land use classifications using five different training sample datasets, based on nine common parcel features and all thirteen parcel features (including four GSV-derived parcel features), respectively.

Random Seed	GSV-derived parcel features		Overall Accuracy (%)	Producer's Accuracy (%)							User's Accuracy (%)						
				Class													
				L1	**L2**	**L3**	**L4**	**L5**	**L6**	**L7**	**L1**	**L2**	**L3**	**L4**	**L5**	**L6**	**L7**
611	No	Value	75.9	92.4	48.0	21.3	40.8	59.2	71.0	13.9	81.2	63.4	44.1	57.8	66.3	65.3	28.2
	Yes	Value	77.2	93.7	46.6	20.4	52.7	59.6	68.7	10.5	81.7	65.8	46.3	65.6	66.7	66.7	26.2
		Improvement	1.4	1.3	-1.3	-0.9	11.9	0.5	-2.3	-3.3	0.5	2.4	2.2	7.8	0.4	1.4	-2.0
1924	No	Value	76.7	92.6	50.2	17.9	42.4	62.0	71.4	11.5	81.9	64.5	48.8	56.7	64.7	70.4	38.2
	Yes	Value	77.8	93.5	49.2	16.4	52.7	62.3	72.9	12.8	82.2	66.0	47.5	64.6	68.8	72.1	46.0
		Improvement	1.1	0.9	-1.0	-1.5	10.3	0.3	1.5	1.3	0.3	1.4	-1.3	8.0	4.1	1.7	7.8
3391	No	Value	76.3	92.2	50.6	19.8	42.3	57.0	61.8	20.6	81.9	63.8	44.8	58.7	61.9	75.2	30.7
	Yes	Value	77.6	93.0	51.0	18.9	51.6	58.1	63.9	19.1	82.5	65.2	49.2	66.9	64.8	74.9	31.7
		Improvement	1.3	0.7	0.4	-0.9	9.3	1.1	2.1	-1.4	0.6	1.4	4.4	8.2	2.9	-0.3	1.0
6763	No	Value	76.4	92.1	49.7	16.1	40.2	66.8	71.5	19.1	81.9	62.7	56.1	58.2	63.2	71.0	36.4
	Yes	Value	77.7	93.0	50.3	15.2	50.0	65.5	69.3	18.2	82.6	64.1	54.7	68.5	64.8	69.1	35.7
		Improvement	1.3	0.9	0.6	-0.9	9.7	-1.3	-2.2	-0.9	0.7	1.4	-1.4	10.3	1.7	-1.9	-0.8
9930	No	Value	76.1	91.7	50.6	18.6	40.9	61.3	67.5	20.7	81.9	62.6	49.6	58.2	63.5	64.9	34.6
	Yes	Value	77.2	92.5	50.2	15.9	49.9	62.5	67.9	19.8	82.5	63.6	52.0	66.8	63.2	62.6	35.5
		Improvement	1.1	0.8	-0.4	-2.7	9.0	1.2	0.4	-0.9	0.6	1.0	2.4	8.5	-0.2	-2.3	0.9
Average	No	Value	76.3	92.2	49.8	18.7	41.3	61.2	68.7	17.2	81.7	63.4	48.7	57.9	63.9	69.4	33.6
	Yes	Value	77.5	93.1	49.5	17.4	51.4	61.6	68.6	16.1	82.3	64.9	49.9	66.5	65.7	69.1	35.0
		Improvement	1.2	0.9	-0.4	-1.4	**10.0**	0.4	-0.1	-1.1	0.5	1.5	1.2	**8.6**	1.8	-0.3	1.4

* **L1**: Single-family house; **L2**: Multi-family residential building; **L3**: Public facility & institution; **L4**: Mixed residential & commercial building; **L5**: Commercial & industrial building; **L6**: Park & open space; **L7**: Parking facility.

Table 5
Confusion matrices for land use classifications using the training sample dataset randomly selected by the random seed 611, based on nine common parcel features and all thirteen parcel features (including GSV-derived parcel features), respectively.

		Reference truth data								
	Class	L1	L2	L3	L4	L5	L6	L7	Total	User Accuracy (%)
Without GSV-derived parcel features	L1	11930	1993	62	548	70	39	58	14700	81.2
	L2	766	2035	89	280	34	1	6	3211	63.4
	L3	11	22	71	11	36	2	8	161	44.1
	L4	160	173	20	603	74	0	13	1043	57.8
	L5	10	12	85	33	368	2	45	555	66.3
	L6	25	7	4	1	12	186	50	285	65.3
	L7	8	1	3	2	28	32	29	103	28.2
	Total	12910	4243	334	1478	622	262	209	20058	
	Producer Accuracy (%)	92.4	48.0	21.3	40.8	59.2	71.0	13.9		
	Overall Accuracy: 75.9%									
		Reference truth data								
	Class	L1	L2	L3	L4	L5	L6	L7	Total	User Accuracy (%)
With GSV-derived parcel features	L1	12094	2059	63	414	63	50	64	14807	81.7
	L2	647	1979	89	241	42	2	7	3007	65.8
	L3	11	17	68	7	33	1	10	147	46.3
	L4	120	167	24	779	85	1	11	1187	65.6
	L5	8	10	84	33	371	1	49	556	66.7
	L6	22	9	3	0	10	180	46	270	66.7
	L7	8	2	3	4	18	27	22	84	26.2
	Total	12910	4243	334	1478	622	262	209	20058	
	Producer Accuracy (%)	93.7	46.6	20.4	52.7	59.6	68.7	10.5		
	Overall Accuracy: 77.2%									

* **L1**: Single-family house; **L2**: Multi-family residential building; **L3**: Public facility & institution; **L4**: Mixed residential & commercial building; **L5**: Commercial & industrial building; **L6**: Park & open space; **L7**: Parking facility.

4.2 Classification Results Using All Thirteen Parcel Features

Fig. 10(a) shows the land use classification based on all the selected thirteen parcel features (including four GSV-derived features) from training samples randomly selected using the random seed number 611. Fig. 10(b) shows incorrectly classified land use class labels (also see Table 4). The average OA of land use classifications is 77.5%. Like the land-use classifications based on the nine parcel features, the single-family house land-use class has the highest producer's and user's accuracies. The park & open space class and the commercial & industrial building class have the second and third highest producer's and user's accuracies, respectively. Average producer's and user's accuracies for public facilities & institutions are 17.4% and 49.9%, respectively. Parking facilities show the lowest classification accuracies, with only 16.1% and 35% for average producer's and user's accuracies, respectively (Table 4).

Although the contribution of GSV-derived parcel features to the average OA improvement is not much (only 1.2% or so) due to a variety of possible reasons (e.g., chosen method for automatic detection and recognition of texts from images, chosen extracted features), their contributions to the producer's accuracy and user's accuracy of the mixed residential & commercial building class are quite high (10 percentage points and 8.6 percentage points, respectively). Therefore, the producer's and user's

accuracies of mixed residential & commercial buildings are even higher than those of multi-family residential buildings after GSV-derived parcel features are incorporated into classification (Table 4). As Table 5 shows, given selected training samples with the random seed 611, producer's and user's accuracies for mixed residential & commercial buildings based on nine common parcel features are 40.8% and 57.8%, respectively, and those based on thirteen parcel features (with GSV-derived parcel features) are 52.7% and 65.6%, respectively. According to the parcel boundaries data, there were 1478 mixed residential & commercial buildings parcels. When only the nine parcel features were used as input features, 548 mixed residential & commercial buildings parcels were misclassified as single-family houses, and 280 were misclassified as multi-family residential buildings. With the four GSV-derived parcel features, 176 misclassifications were corrected, among which 134 were from misclassified single-family house parcels and 39 were from misclassified multi-family residential building parcels (Table 5).

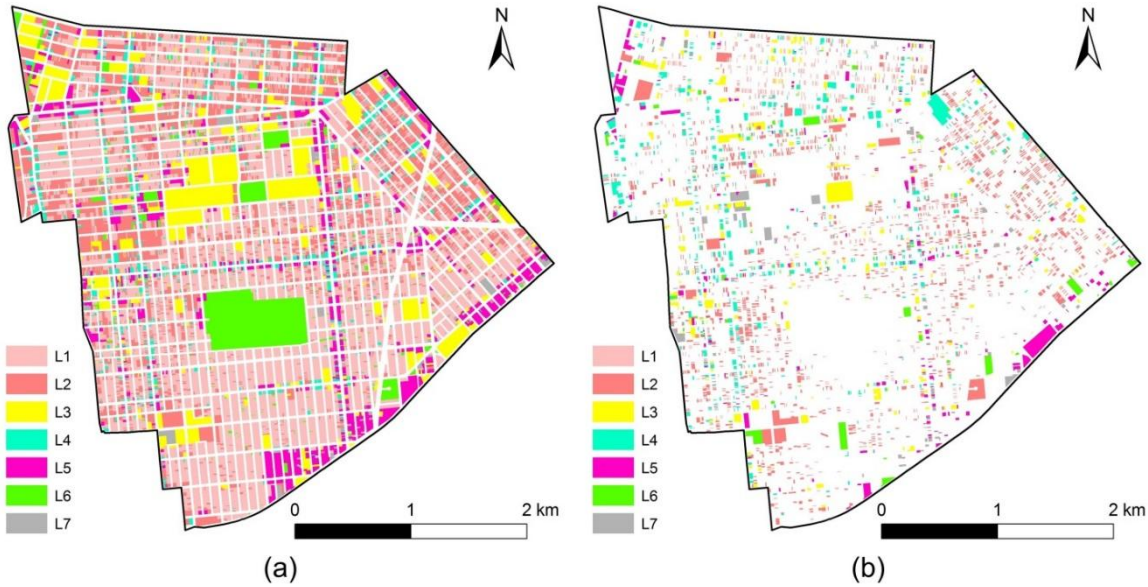

Fig. 10. (a) Land use classification based on all selected thirteen parcel features, including GSV-derived parcel features, and the training samples randomly selected using the random seed number 611. (b) Corresponding land use misclassification.

4.3 Parcel Features Importance Evaluation

The feature importance was evaluated by the depth of a feature used as a decision node in a tree. In other words, the top of the tree impacts a larger fraction of the input samples in terms of final classification than the bottom part of the tree (Pedregosa et al., 2011). The blue bars in Fig. 11 show the feature importance values of the thirteen parcel features in the random forest, along with their inter-trees variability values, which were calculated as STDs from feature importance evaluation of classifications based on 5 different random seeds. STD of building story numbers (PF-7), STD of building areas (PF-4), and number of buildings (PF-2) were the three least important features used in classification. Because in the study area parcels with single building are common, STD of building story numbers and STD of building areas are just zero and number of buildings is just 1 for most of parcels. Maximum of building areas (PF-3), percentage of total building area (PF-5), and parcel size (PF-1) are the three most significant features. The significance of PF-5 (percentage of total building area) may explain why both average of NDVI (PF-8) and STD of NDVI (PF-9) are also influential due to the fact that the latter are complementary to the former. Compared to other parcel features, in this study the selected parcel features derived from GSV images (PF-10 to PF-13) are not very significant in decision tree building. Detected text at a smaller horizontal field view angle is more important than that at a larger view angle. Referring to the results above, GSV-derived parcel features are only important in improving the classification accuracy of the mixed residential & commercial building parcels.

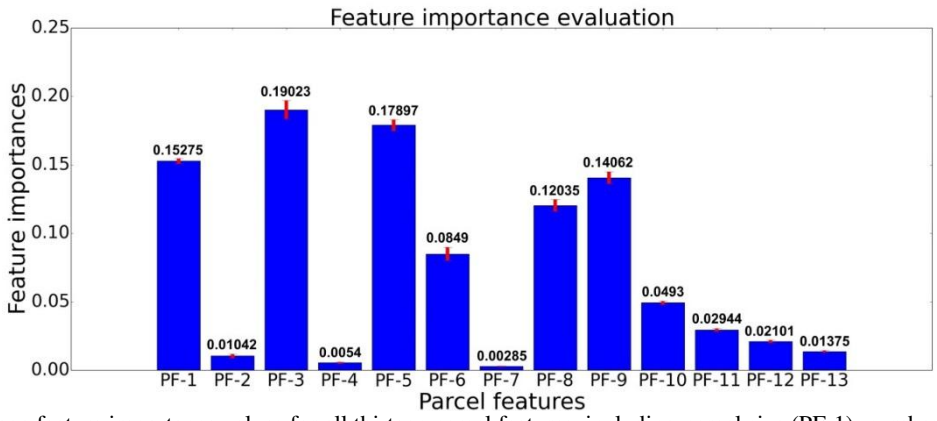

Fig. 11. Average feature importance values for all thirteen parcel features, including parcel size (PF-1), number of buildings (PF-2), maximum of building areas (PF-3), STD of building areas (PF-4), percentage of total building area (PF-5), maximum of building story numbers (PF-6), STD of building story numbers (PF-7), average of NDVI (PF-8), STD of NDVI (PF-9), length of detected text from *fov* 30 GSV image (PF-10), length of detected text from *fov* 45 GSV image (PF-11), length of detected text from *fov* 60 GSV image (PF-12), and index of English word from all detected texts (PF-13).

In order to further test the effectiveness of GSV for improving accuracy of land use classification under a complex megacity background, we made a comparison between land use classification based on only six relatively important common parcel features (no GSV-derived parcel features) and land use classification based on the six relatively important common parcel features and the GSV-derived parcel features (Table 6). Removing the three least important features (STD of building story numbers, STD of building areas, and number of buildings) only makes a small difference. Contributions of GSV-derived parcel features to the producer's accuracy and user's accuracy of mixed residential & commercial buildings are still high (12.1% and 8.4%, respectively) (Table 6).

Table 6
Confusion matrices for land use classifications using the training sample dataset randomly selected by the random seed 611, based on six relatively important common parcel features (PF-1, PF-3, PF-5, PF-6, PF-8, and PF-9) and these important common parcel features plus GSV-derived four parcel features, respectively.

		Reference truth data								
	Class	L1	L2	L3	L4	L5	L6	L7	Total	User Accuracy (%)
Without GSV-derived parcel features	L1	11966	2011	62	542	73	47	63	14764	81.0
	L2	740	2011	86	280	37	0	6	3160	63.6
	L3	14	25	73	13	25	1	8	159	45.9
	L4	153	177	23	607	78	1	11	1050	57.8
	L5	6	12	82	34	371	2	49	556	66.7
	L6	21	6	3	0	11	180	43	264	68.2
	L7	10	1	5	2	27	31	29	105	27.6
	Total	12910	4243	334	1478	622	262	209	20058	
	Producer Accuracy (%)	92.7	47.4	21.9	41.1	59.6	68.7	13.9		
	Overall Accuracy: 76%									

		Reference truth data									
	Class	L1	L2	L3	L4	L5	L6	L7	Total	User Accuracy (%)	User Accuracy Improvement (%)
With GSV-derived parcel features	L1	12083	2026	59	399	64	47	64	14742	82.0	0.9
	L2	670	2014	90	252	40	1	7	3074	65.5	1.9
	L3	7	22	66	7	34	1	5	142	46.5	0.6
	L4	115	164	27	786	82	1	13	1188	66.2	8.4

L5	7	9	84	29	370	2	50	551	67.2	0.4
L6	20	6	3	0	12	178	42	261	68.2	0.0
L7	8	2	5	5	20	32	28	100	28.0	0.4
Total	12910	4243	334	1478	622	262	209	20058		
Producer Accuracy (%)	93.6	47.5	19.8	53.2	59.5	67.9	13.4			
Producer Accuracy Improvement (%)	0.9	0.1	-2.1	12.1	-0.2	-0.8	-0.5			
Overall Accuracy: 77.4%										
Overall Accuracy Improvement: 1.4%										

* **L1**: Single-family house; **L2**: Multi-family residential building; **L3**: Public facility & institution; **L4**: Mixed residential & commercial building; **L5**: Commercial & industrial building; **L6**: Park & open space; **L7**: Parking facility.

5. Discussion

5.1 Land Use Classification in Megacity

The complexity of the megacity landscape may explain the relative low classification accuracies for some land use classes. For example, multi-family residential buildings in megacities are commonly single two-flat, three-flat, or four-flat buildings. In other sizes of cities, parcels for multi-family residential buildings tend to consist of a multi-story large building or a group of townhouses. Compared with the accuracies of public facility & institution in Wu et al. (2009) and Hu and Wang (2013), it is not surprising that the public facility & institution land use class has low classification accuracy in this study of a megacity using only remotely sensed data, because public facility & institution land use is mainly a social function. Parking facility is another land use class with very low accuracy, which may be caused by its confusing use definition. In reality, a garage, towing company, bus station or even an auto shop can be classified as parking facilities. Table 5 shows that among the 209 parcels for the parking facility class, 64 parcels were misclassified as single-family houses, 49 parcels were misclassified as commercial & industrial buildings, and 22 parcels were misclassified as park & open space. Comparing land use information from the parcel boundary dataset to Google Maps shows that some parking facility parcels include garages, car towing services, car dealers, outdoor large parking lots, and small parking lots. This may explain most of the classification errors for parking facilities as due to their misclassifications as single-family houses, commercial & industrial buildings, and park & open space.

5.2 Using Text Information from GSV Images in Land Use Classification

Although the contributions of parcel features from GSV images to the producer's accuracy and user's accuracy of the mixed residential & commercial building class are high (10 percentage points and 8.6 percentage points, respectively), the average OA improvement for all classes is not very much because the impacted classes (mainly the mixed residential & commercial building parcels) account for a small proportion of all land use parcels. Although the single-family house class has a high accuracy, multi-family residential building, public facility & institution, and parking facility together reduce the average OA. In addition, in reality, detected texts by GSV images can also include other kinds of signs other than shop signs on mixed residential & commercial buildings, such as car-relevant business signs, church signs, and day-care signs (Fig. 12). This may explain why the user's accuracy of public facilities & institutions is improved by just 1.8 percentage points on average (Table 4), and why there are only slight accuracy increases and decreases for other land use classes. In addition, because of the complexity, low quality, and varying brightness of GSV images, it is still challenging to automatically derive correct texts from GSV images. This is also considered as a major barrier to classifying land use based on detected texts, because OCR performs best only when the text is located on a uniform background and is formatted like a document.

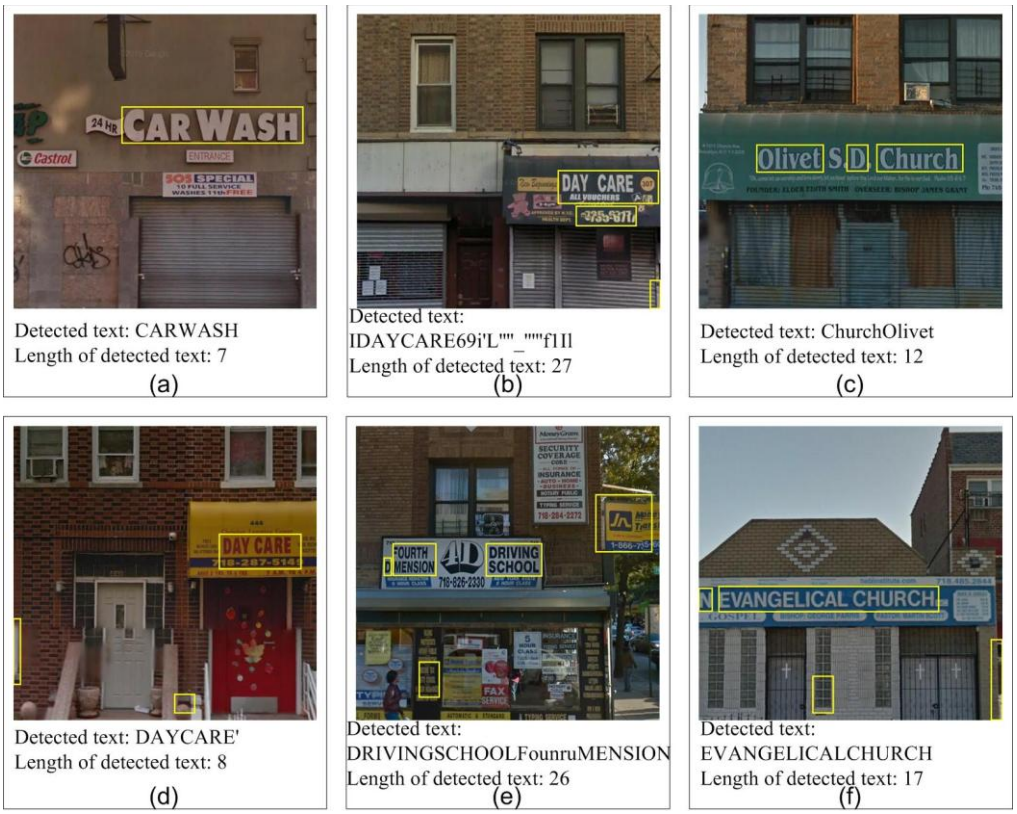

Fig. 12. Detected texts from GSV images for public facilities & institutions.

6. Conclusions

A case study using parcel features, including GSV-derived features, for parcel-level urban land use classification in a megacity area is presented. This case study shows that: (1) parcel-based urban land-use classification in a megacity by RF classifier using airborne LiDAR, HRO, and GSV is capable of distinguishing single-family houses from other buildings at an average accuracy of over 90%, even with the complexity of a megacity landscape; and commercial & industrial buildings and park & open space also can have relatively high classification accuracies using these data in concert; (2) among the thirteen used parcel attributes, parcel size, maximum of building areas, percentage of total building area, average of NDVI, and STD of NDVI are the five most important parcel features for classification; (3) the parcel features derived from GSV images can largely contribute to the producer's accuracy and user's accuracy of mixed residential & commercial buildings, with 10 percent and 8.6 percent improvement, respectively.

Compared to previous relevant work, this study indicates that parcel-based urban land-use classification using only remotely-sensed data with RF classifier can produce accurate classification of single-family houses and relatively accurate classification of multi-family residential buildings, mixed residential & commercial buildings, commercial & industrial buildings, and park & open space on a megacity landscape. In particular, this study demonstrates that using text information derived from GSV images may be an important aid in distinguishing between some related land-use classes, particularly mixed residential & commercial building, and others.

References

Anderson, J. R. (1976). *A land use and land cover classification system for use with remote sensor data* (Vol. 964). US Government Printing Office. Washington.

Aubrecht, C., Steinnocher, K., Hollaus, M., & Wagner, W. (2009). Integrating earth observation and GIScience for high resolution spatial and functional modeling of urban land use. *Computers, Environment and Urban Systems*, *33*(1), 15-25.

503 Barnsley, M. J., & Barr, S. L. (1997). Distinguishing urban land-use categories in fine spatial resolution land-cover
504 data using a graph-based, structural pattern recognition system. *Computers, Environment and Urban*
505 *Systems*, *21*(3), 209-225.
506 Barr, S., & Barnsley, M. (2000). Reducing structural clutter in land cover classifications of high spatial resolution
507 remotely-sensed images for urban land use mapping. *Computers & Geosciences, 26*(4), 433-449.
508 Bauer, T., & Steinnocher, K. (2001). Per-parcel land use classification in urban areas applying a rule-based
509 technique. GeoBIT/GIS, 6, 24-27.
510 Bentley, G., McCutcheon, P., Cromley, R. & Hanink, D (2016). Fitzgerald: A return to the neighborhood and its
511 contemporary structural and geographical contexts. *The Professional Geographer*. 68(3), 414-426
512 Breiman, L. (2001). Random forests. *Machine learning, 45*(1), 5-32.
513 Cox, W. (2015). Demographia World Urban Areas. 12th Annual Edition. http://www.Demographia.com/db-
514 worldua.pdf Accessed 16.04.
515 Donnay, J. P., & Unwin, D., (2001). Modeling geographical distributions in urban areas. In J. P. Donnay, M. J.
516 Barnsley, & P. A. Longley (Eds.), *Remote sensing and urban analysis* (pp. 205–24). New York: Taylor &
517 Francis.
518 Gislason, P. O., Benediktsson, J. A., & Sveinsson, J. R. (2004, September). Random forest classification of
519 multisource remote sensing and geographic data. *In Geoscience and Remote Sensing Symposium, 2004.*
520 *IGARSS'04. Proceedings. 2004 IEEE International* (Vol. 2, pp. 1049-1052). IEEE.
521 Google. (2016). Google Street View Image API.
522 https://developers.google.com/maps/documentation/streetview/intro Accessed 16.08.05.
523 Grus, J. (2015). *Data Science from Scratch: First Principles with Python*. (1st ed.). Sebastopol: O'Reilly Media.
524 Hara, K., Le, V., & Froehlich, J. (2013, April). Combining crowdsourcing and google street view to identify street-
525 level accessibility problems. *In Proceedings of the SIGCHI conference on human factors in computing systems*
526 (pp. 631-640). ACM.
527 Herold, M., Liu, X., & Clarke, K. C. (2003). Spatial metrics and image texture for mapping urban land use.
528 *Photogrammetric Engineering & Remote Sensing, 69*(9), 991-1001.
529 Hu, S., & Wang, L. (2013). Automated urban land-use classification with remote sensing. *International Journal of*
530 *Remote Sensing, 34*(3), 790-803.
531 Li, X., Meng, Q., Li, W., Zhang, C., Jancso, T., & Mavromatis, S. (2014). An explorative study on the proximity of
532 buildings to green spaces in urban areas using remotely sensed imagery. *Annals of GIS, 20*(3), 193-203.
533 Li, X., Zhang, C., Li, W., Ricard, R., Meng, Q., & Zhang, W. (2015). Assessing street-level urban greenery using
534 Google Street View and a modified green view index. *Urban Forestry & Urban Greening, 14*(3), 675-685.
535
536 Liu, X. (2008). Airborne LiDAR for DEM generation: some critical issues. *Progress in Physical Geography, 32*(1),
537 31-49.
538 MathWorks. (2016). Automatically Detect and Recognize Text in Natural Images.
539 http://www.mathworks.com/help/vision/examples/automatically-detect-and-recognize-text-in-natural-
540 images.html Accessed 16.07.25.
541 Moller-Jensen, L. (1997). Classification of urban land cover based on expert systems, object models and
542 texture. *Computers, environment and urban systems*, *21*(3), 291-302.
543 New York City Department of City Planning. (2016a). MapPLUTO METADATA.
544 http://www1.nyc.gov/assets/planning/download/pdf/data-maps/open-data/meta_mappluto.pdf Accessed
545 16.06.02.
546 New York City Department of City Planning. (2016b). New York City Community Districts Metadata.
547 http://www1.nyc.gov/assets/planning/download/pdf/data-maps/open-data/nycd_metadata.pdf?v=16b Accessed
548 16.06.02.
549 NOAA. (2015). 2013-2014 U.S. Geological Survey CMGP LiDAR: Post Sandy (New York City).
550 https://data.noaa.gov/harvest/object/318b34e9-622c-4329-9a92-95a7b2a158f0/html/original Accessed 16.07.05.
551 Pedregosa, F., Varoquaux, G., Gramfort, A., Michel, V., Thirion, B., Grisel, O., Blondel, M., Prettenhofer, P., Weiss,
552 R., Dubourg, V. and Vanderplas, J. (2011). Scikit-learn: Machine learning in Python. *Journal of Machine*
553 *Learning Research, 12*(Oct), 2825-2830.
554 Platt, R. V., & Rapoza, L. (2008). An Evaluation of an Object-Oriented Paradigm for Land Use/Land Cover
555 Classification∗. *The Professional Geographer, 60*(1), 87-100.
556 Priestnall, G., Jaafar, J., & Duncan, A. (2000). Extracting urban features from LiDAR digital surface
557 models. *Computers, Environment and Urban Systems*, *24*(2), 65-78.

Rodriguez-Galiano, V. F., Ghimire, B., Rogan, J., Chica-Olmo, M., & Rigol-Sanchez, J. P. (2012). An assessment of the effectiveness of a random forest classifier for land-cover classification. *ISPRS Journal of Photogrammetry and Remote Sensing, 67*, 93-104.

Rundle, A. G., Bader, M. D., Richards, C. A., Neckerman, K. M., & Teitler, J. O. (2011). Using Google Street View to audit neighborhood environments. *American journal of preventive medicine, 40*(1), 94-100.

Song, C. (2005). Spectral mixture analysis for subpixel vegetation fractions in the urban environment: How to incorporate endmember variability? *Remote Sensing of Environment, 95*(2), 248-263.

Treitz, P. M., Howarth, P. J., & Gong, P. (1992). Application of satellite and GIS technologies for land-cover and land-use mapping at the rural-urban fringe: a case study. *Photogrammetric engineering and remote sensing, 58*(4), 439-448.

Tucker, C. J. (1979). Red and photographic infrared linear combinations for monitoring vegetation. *Remote sensing of Environment, 8*(2), 127-150.

U.S. Census Bureau. (2016). Annual Estimates of the Resident Population for Incorporated Places of 50,000 or More, Ranked by July 1, 2015 Population: April 1, 2010 to July 1, 2015. http://factfinder.census.gov/faces/tableservices/jsf/pages/productview.xhtml?src=bkmk Accessed 16.09.25.

Version, L. S. (2009). Version 1.3–R10. *The American Society for Photogrammetry & Remote Sensing (ASPRS)*.

Wentz, E. A., Stefanov, W. L., Gries, C., & Hope, D. (2006). Land use and land cover mapping from diverse data sources for an arid urban environments. *Computers, Environment and Urban Systems*, *30*(3), 320-346.

Winters, F. (2016). StreetSegment Public Geospatial_Data_Presentation_Form: vector digital data. http://gis.ny.gov/gisdata/metadata/nysgis.streets_public.xml Accessed 16.08.01.

Worldatlas. (2016). Populations Of 150 Largest Cities In The World. http://www.worldatlas.com/citypops.htm Accessed 16.08.01.

Wu, S., Qiu, X., Usery, E. L., & Wang, L. (2009). Using geometrical, textural, and contextual information of land parcels for classification of detailed urban land use. *Annals of the Association of American Geographers, 99*(1), 76-98.

Wu, S., Silván-Cárdenas, J., & Wang, L. (2007). Per-field urban land use classification based on tax parcel boundaries. *International Journal of Remote Sensing, 28*(12), 2777-2801.